

Nano-structured metallic electrodes for plasmonic optimized light-emitting diodes

U. Geyer^a, J. Hetterich^a, C. Diez^a, D. Z. Hu^b, D. M. Schaadt^b, and U. Lemmer^a

^a Universität Karlsruhe (TH), Light Technology Institute (LTI), Kaiserstr.12, 76131 Karlsruhe, Germany

^b Universität Karlsruhe (TH), Institute for Applied Physics, Kaiserstr.12, 76131 Karlsruhe, Germany

ABSTRACT

Metallic nanostructures have attracted large interest recently due to new optical properties caused by plasmonic effects. The exceptionally high transmission of light through periodically structured metals is originated by interactions between light and plasmonic resonances. These resonances are controllable by varying periodicity and geometrical dimensions of the metal gratings.

Our aim is the utilization of these effects to improve the efficiency of conventional light-emitting diodes (LED). The application of one-dimensional periodic metallic gratings as top electrodes of LEDs offers advantages such as efficient and homogeneous current injection, enhanced light output, modified angular light emission characteristics and linear polarization of the emission.

Based on finite-difference time-domain simulations, we optimized the parameters for gold and silver gratings on top of InGaAs/GaAs/AlAs heterostructures. Fabrication of these structures was carried out using laser interference lithography (LIL) and a lift-off process. We measured the optical transmission of these structures and were able to demonstrate a polarization- and wavelength-dependence in good consistency with our calculations.

Keywords: Light-emitting diode, Surface plasmons, Laser interference lithography

1. INTRODUCTION

Although light emitting diodes (LED) have been used successfully for many years as light sources, they have not yet succeeded in replacing conventional illuminants such as fluorescent lamps for domestic lighting. One reason for this, in addition to higher production costs, is the lower energy efficiency of commercially available LEDs compared with well-established gas-discharge lamps [1]. While the internal quantum efficiency, which is the conversion rate of injected electrons into photons, has already improved to high levels, the light extraction efficiency of generated photons has yet to be promoted [2]. Many different approaches of enhancing the external efficiency have been reported in the past, e. g. photonic crystal LEDs [3,4], microcavity LEDs [5], substrate shaping using truncated pyramids [6], as well as the utilization of surface plasmons excited at metal layers on top [7-9] or inside [10,11] the LED.

Our focus here is on a modification of the characteristics of a luminescence diode to achieve an emission into a smaller solid angle to reach higher extraction efficiencies and obtain highly-polarized light for efficient use of the emitted power in optical systems such as LC-displays. To do so we want to apply nano-structured one-dimensional periodic metallic gratings which serve as top electrodes of LEDs. Periodicity and geometrical properties of the grating have to be determined to reach a coupling of the emitted photons with surface plasmons (SP), which can be excited at the corrugated metal surface. This optimization is done with finite-difference time-domain (FDTD) simulations that are shown in section 2. In section 3, we describe our fabrication method to pattern the top electrode using interference lithography and a lift-off process. To test our simulations and fabrication methods, we analyzed the optical transmission through this metal gratings, which is shown in section 4. A conclusion is given in section 5.

2. SIMULATIONS

Surface plasmons are collective excitations of free electrons in metals that propagate along the interface between a conductor and an insulator or semiconductor. Because of different dispersion relations of photons and surface plasmons, it is not possible to excite them directly. The SP wavevector is expressed [12] by

$$k_{SP} = k_0 \sqrt{\frac{\varepsilon_d \varepsilon_m}{\varepsilon_d + \varepsilon_m}},$$

with k_0 the free-space wavevector of light, and ε_d and ε_m the frequency dependent permittivity of the dielectric and the metal, respectively. To enable a coupling between photons and SP, the resulting momentum mismatch has to be adjusted. This can be done by using a prism configuration [13], surface roughnesses [8] or periodic metallic structures [14]. In the case of periodic structures, the wavevector of the photon can be added or subtracted with integer multiples of the grating wavevector:

$$k_{SP} = k_0 \sin \theta \pm nk_g,$$

where $k_0 \sin \theta$ is the in-plane wavevector of light and $k_g = 2\pi / \lambda_g$ is the grating wavevector. The grating periodicity λ_g has to be in the order of the wavelength of the photons. With one-dimensional periodic structures, surface plasmons can only be excited by p-polarized photons with the electrical field vector perpendicular to the grating grooves. S-polarized photons should not couple to the plasmons.

The applications of periodic metal gratings combined with LEDs have already been reported. In [7, 15] the changed angular distribution was shown with inorganic LEDs, in [16] with organic LEDs. We simulated the effect of a metal grating on top of a conventional GaAs-based LED with respect to total efficiency and angular light emission characteristics. We applied the FDTD-method using the commercially available software LUMERICAL¹. As shown in Fig. 1(a), the total emitted power is considerably enhanced by a factor of 3 at the emission wavelength of 958 nm. In Fig. 1(b), the angular distribution in the far field at the peak wavelength of 958 nm is illustrated. As expected, the s-polarized light is hindered from emission by the metal grating, whereas the p-polarized light is intensified especially at a small angle distribution of 15 degrees around the forward direction.

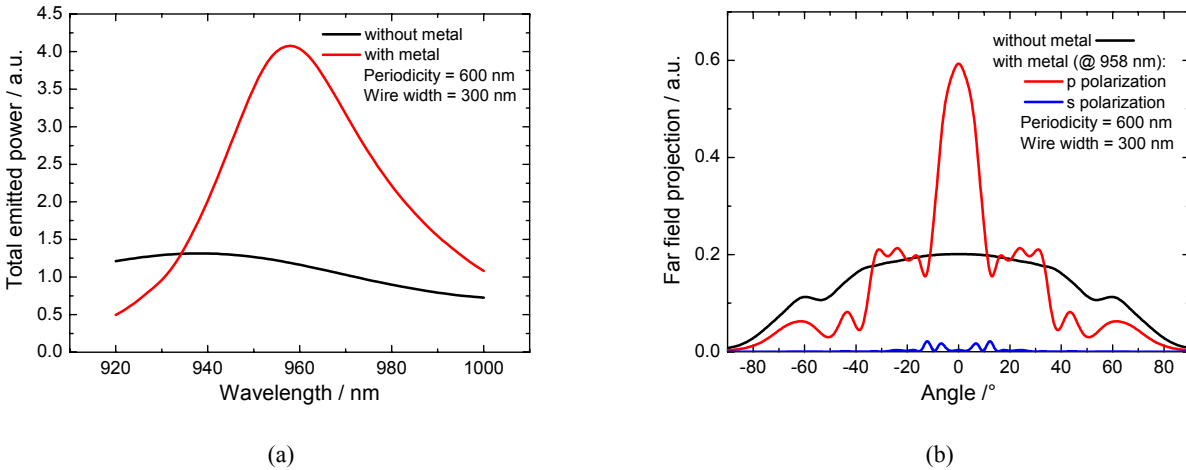


Fig. 1. (a) Simulation of the enhancement of the total emitted power by applying a metal grating on top of an LED. (b) Changed angular distribution of this nano-structured LED compared to a conventional LED.

To reveal the effect of different grating parameters, we varied the periodicity, the thickness and the width of the metal stripes. Optimization was done with a test structure shown in Fig. 2, consisting of 300-nm-thick GaAs on top of an 800-nm-thick AlAs layer. Because of the lower refractive index of AlAs of 2.9 compared to GaAs of 3.4, this structure

¹ <http://www.lumerical.com>

forms a waveguide with guided modes underneath the surface. This leads to a higher density of the electromagnetic field close to the surface and therefore to an increased interaction between the plasmonic modes of the metal grating and light. The thicknesses of the GaAs and AlAs layers were optimized for maximal coupling between the plasmons and the guided modes. After fabrication of the structure, the thicknesses of all layers were determined by ellipsometric measurements. The substrate used for this experiment consisted of 817 nm AlAs, 270 nm GaAs and a top layer of 2.6 nm GaAs-oxide.

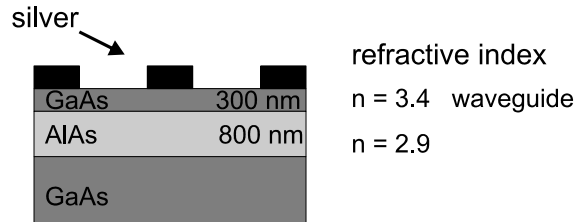
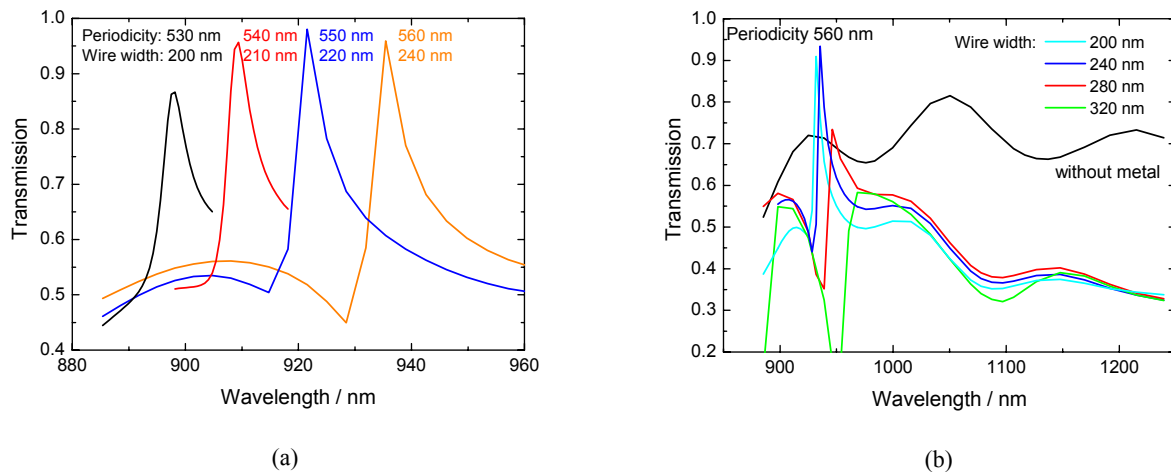
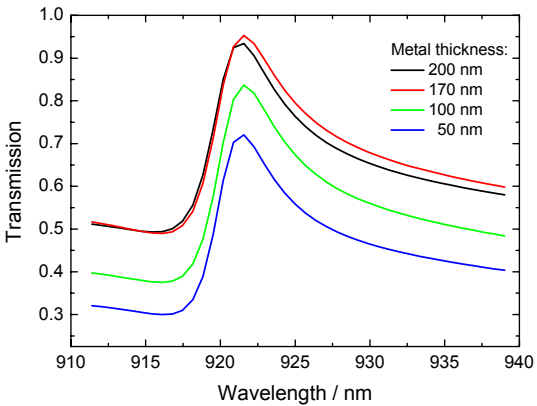


Fig. 2. Design for optimization of the grating parameters.

As seen in Fig. 3(a), a change in the periodicity results in a shift of the plasmonic resonance. By varying the periodicity between 530 nm and 560 nm, we are able to tune the resonance in the transmitted light from 900 to 940 nm. In this way, periodicity will be used for matching the transmission peak to the emission spectrum of the LED. The influence of the wire width is shown in Fig. 3(b). By varying the wire width, the coupling between plasmons localized on the individual wires can be controlled. Changing the width from 200 nm to 320 nm at a fixed periodicity of 560 nm will cause large differences in the transmission spectra. To obtain an enhanced transmission compared to an unstructured sample, the wire width must not leave a narrow range around the optimum. Therefore, the determination of the optimum width will be crucial for the success of a plasmonic enhanced LED. This is also a serious demand on the fabrication, especially to the reproducibility of interference lithography. The last important parameter is the metal thickness, due to the coupling between SPs on the top- and bottom-surfaces of the metallic wires. The effect of different grating thicknesses is displayed in Fig. 3(c). Increasing the metal thickness will lead to a rise of transmission. The optimum is reached at 170 nm; beyond this point the transmission is decreasing. We also found that there is only a slight difference between gold and silver gratings. This can be explained by similar dielectric functions of both metals in this spectral range. According to our simulations, the transmission through GaAs can be enhanced up to 95% with a 170 nm thick metal grating compared to 70% of an unstructured sample.





(c)

Fig. 3. Simulated transmission of silver gratings on GaAs/AlAs structure using FDTD-method. Variation of (a) periodicity, (b) stripe width and (c) metal thickness.

3. FABRICATION

Fabrication of GaAs/AlAs-heterostructures was conducted using Molecular-beam Epitaxy (MBE). In this article, our focus is on the fabrication of metal structures.

One option to produce large-scale metal gratings is laser interference lithography (LIL). Unlike electron beam lithography, this is a method that enables rapid fabrication of large areas with high accuracy in the periodicity. The fundamental idea is based on the interference of two laser beams which results in a periodic light pattern of dark and bright lines (see Fig. 4). The periodicity Λ of the pattern can be defined by the incident angle θ of the beams and is calculated by the formula $\Lambda = \lambda / (2 \sin \alpha)$.

Our setup uses a cw-Ar⁺-Laser (Coherent Innova Sabre TSM 5) operating at a wavelength of 363.8 nm (see Fig. 5). The laser beam is split into two equal parts that are cleaned up by spatial filters. Afterwards the expanded beams are superposed on the sample. By varying the angle of the beams, we are able to change the periodicity of the interference grating between 300 and 800 nm.

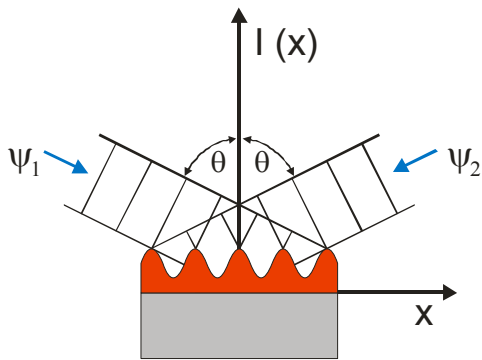


Fig. 4. Superposition of two plane waves results in an interference pattern, which can be used for exposure of photoresist.

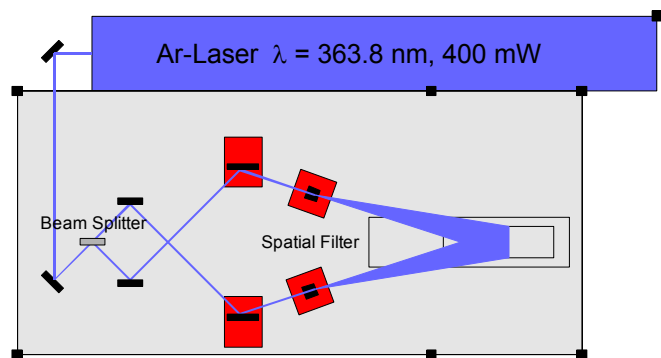


Fig. 5. Setup for laser interference lithography.

The processing of the samples is divided into four steps (see Fig. 6). First, the samples are coated with UV-sensitive positive tone photoresists (Allresist AR-P 3120 or Allresist AR-P 3170) with layer thicknesses of 600 and 200 nm respectively (step 1). Both thicknesses were compared in terms of evaluating which layer thickness is appropriate to produce photoresist gratings and to examine the feasibility of the lift-off process. Then the samples are exposed in the laser interference lithography setup (step 2). The exposure doses of the resists are 40 mJ/cm². Development is done with Allresist AR 300-35; different dilutions of the developer with water lead to a change in the duty cycle (see Fig. 7). The duty cycle defines the width of the metal stripes. As shown in section 2, this parameter is important for the function of the grating. Therefore, much attention must be given to it.

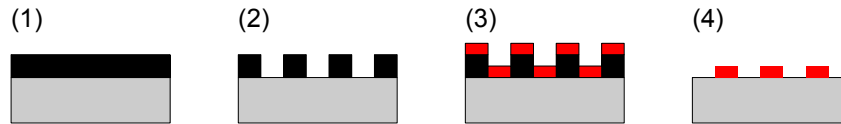


Fig. 6. Processing steps (1) photoresist deposition (2) light exposure and development (3) thermal evaporation of silver/gold (4) lift-off.

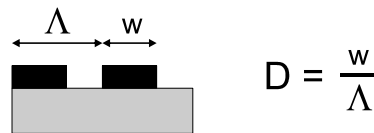


Fig. 7. Definition of the duty cycle.

After development we obtain a photoresist mask that can be used for the following lift-off process. In the Figures 8(a) and (b), SEM micrographs of the cross-sections with photoresist thicknesses of 200 and 600 nm are shown. Standing waves in the direction normal to the sample surface are observable. These are a result of back reflection of the incoming laser beams at the interface between the photoresist layer and the sample surface and have a periodicity of approx. 120 nm in our case [17]. We also managed to structure the 600-nm-thick photoresist, which leads to grating ridges with an aspect ratio of more than 3.

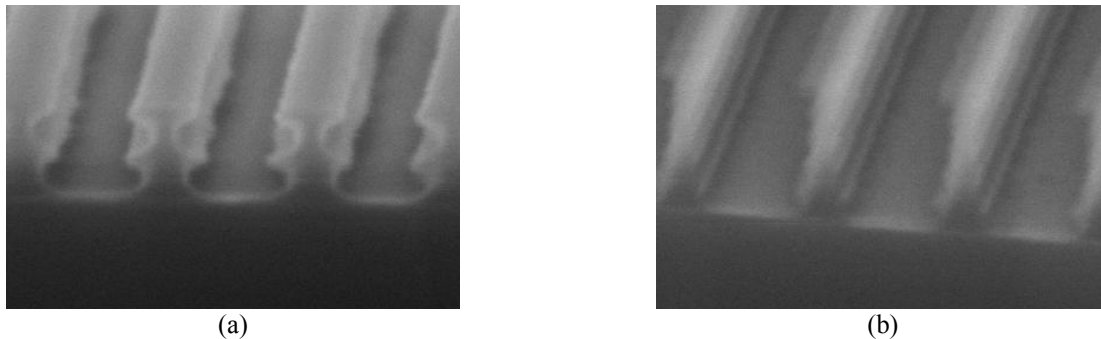


Fig. 8. Photoresist mask of (a) 200 nm and (b) 600 nm thickness.

The third step of the processing is the deposition of the metal. Metallization of gold or silver is done in high vacuum by thermal evaporation. The final step is a lift-off process. The photoresist and covering metal structures are removed in acetone. This can be supported by slight ultrasound, but with high risk of peeling of all structures.

Concluding from the simulations in section 2, the thickness of the metal grating has to be 170 nm. This thickness is challenging for the lift-off (step 4). With 200 nm thick photoresist, we are able to produce metal gratings up to a layer thickness of 90 nm (see Fig. 9). Above this level a clean lift-off is not possible (Fig. 10) because of sticking metal stripes. This can be explained by a metallization of vertical resist structures, which leads to a raised level of adhesion between the metal gratings in the photoresist grooves and the covering metal layer. With a 170 nm thick metal film, we obtain a noteworthy structure shown in Fig. 10(b), consisting of 200 nm high air-tubes surrounded by metal.

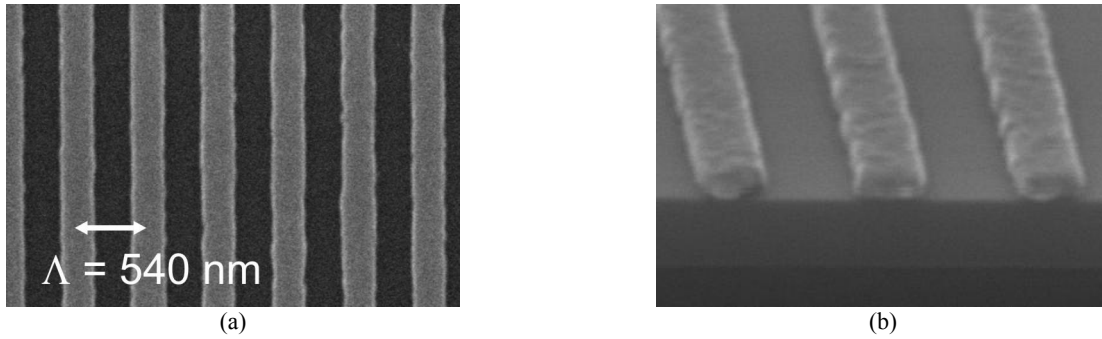


Fig. 9. Metal grating with periodicity of 540 nm and thickness of 80 nm. (a) top view (b) cross-section.

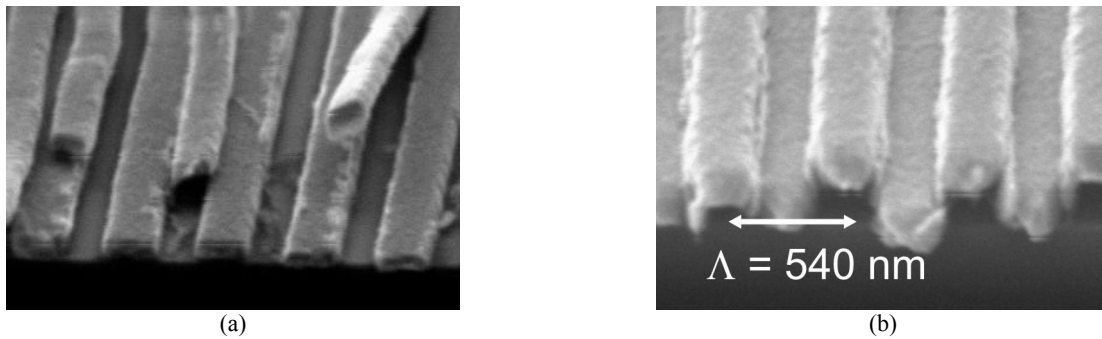


Fig. 10. (a) Metal gratings with thickness of 100 nm and (b) 170 nm. Lift-off is not possible because of thin photoresist thickness.

To avoid the problems shown in Fig. 10, it is necessary to increase the thickness of the photoresist mask. As an alternative, we use a 600-nm-thick resist layer. With higher resist layers a complete development of the photoresist in the grooves is becoming more difficult and irreproducible. After the metallization process, the slope of the resist grating is still covered with metal (see Fig. 11(a)), which inhibits the lifting of the covering metal (Fig. 11 (b)). Ultrasonic assisted lift-off is not recommendable because of low adhesion of gold and silver on top of GaAs.

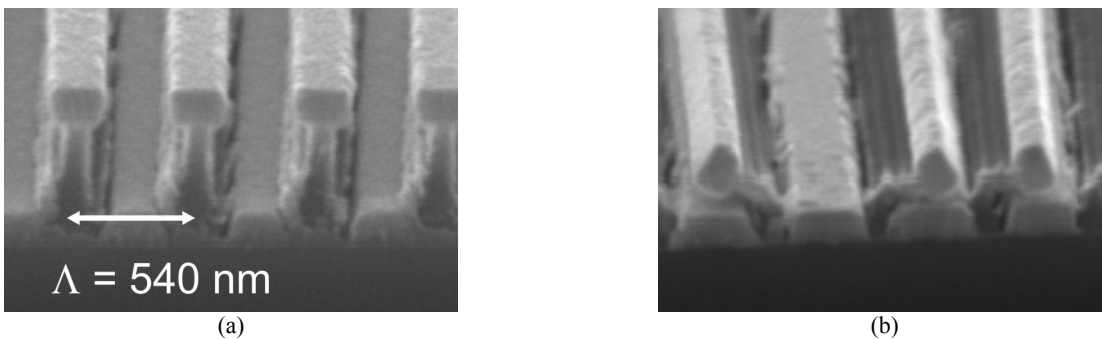


Fig. 11. Lift-off of 170 nm thick gold grating. (a) photoresist mask before and (b) after lift-off. Metallization of the slopes inhibits a lifting of the covering metal.

4. MEASUREMENTS

For testing of our simulation and fabrication methods, we used GaAs substrates with an embedded AlAs layer described in section 2 (Fig.2). On top of this substrate we made silver gratings with a periodicity of 540 nm and layer thicknesses of 60 nm, 80nm and 100 nm.

The measurements were taken using a confocal microscope setup shown in Fig. 12. A halogen lamp serves as a broadband illumination source in the infrared region. The samples are placed between a polarization filter and an aperture on the one hand, and a microscope objective on the other. The transmitted light is analyzed with a spectrograph equipped with a CCD camera. The spatial resolution of the measuring spot is 2.5 μm .

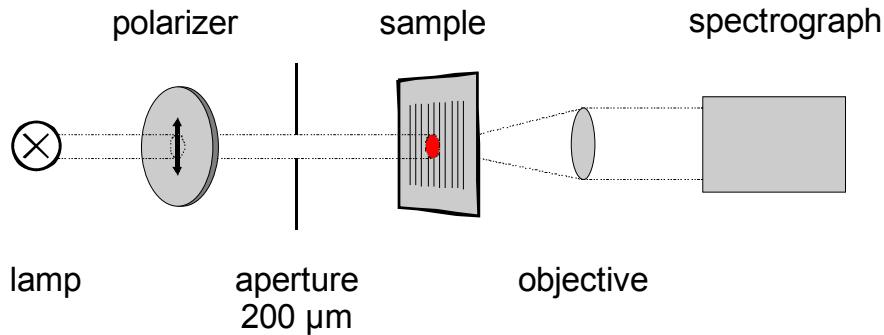
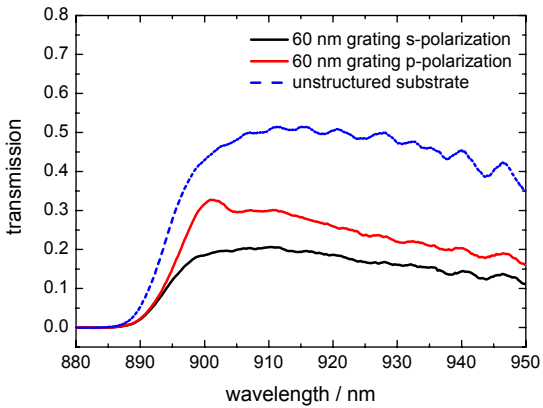


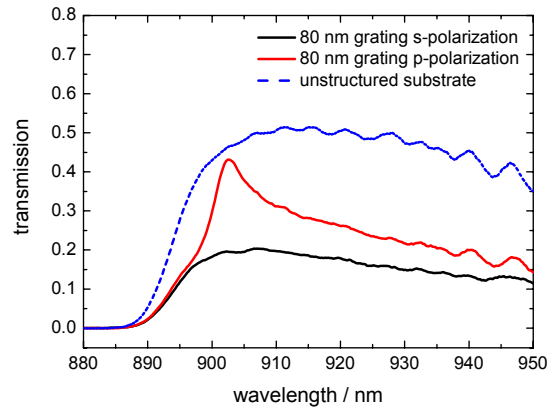
Fig. 12. Setup for transmission measurements of metal gratings on GaAs/AlAs/GaAs heterostructures.

With this setup we were able to detect plasmonic effects caused by the metal grating on top of the GaAs/AlAs/GaAs heterostructure. In Figures 13(a) – (c), the transmission of light through metal gratings in comparison to an unstructured sample are shown. We measured both the polarization of the incoming light parallel to the grating (s-polarization) and perpendicular to the grating (p-polarization). With a grating thickness of 60 nm and 80 nm, a transmission peak at 902 nm in the p-polarized spectrum is clearly observable. Compared to our simulations (see Fig. 14), we found good consistency in the spectral position of the plasmonic resonance as well as in the absolute transmission. It is remarkable that with the 80 nm-thick silver grating the transmission, both with and without grating, is nearly the same. With regard to a metal cover of approx. 45 % of the sample surface, this result is a clear indication of plasmonic effects.

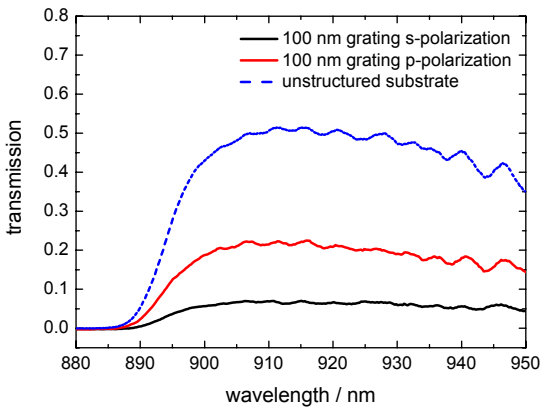
With a metal thickness of 100 nm, we had lift-off problems mentioned in section 3. With this sample the lift-off was not completely realized and some parts of the metal layer covering the photoresist remained on the sample. As shown in Fig. 13(c), this leads to low transmission for both s- and p-polarizations. There is no observable resonance between 900 nm and 910 nm.



(a)



(b)



(c)

Fig. 13 Transmission through (a) 60 nm, (b) 80 nm and (c) 100 nm thick metal grating on top of GaAs/AlAs/GaAs heterostructures. Due to plasmonic effects, the transmission of light with polarization perpendicular to metal grating is enhanced.

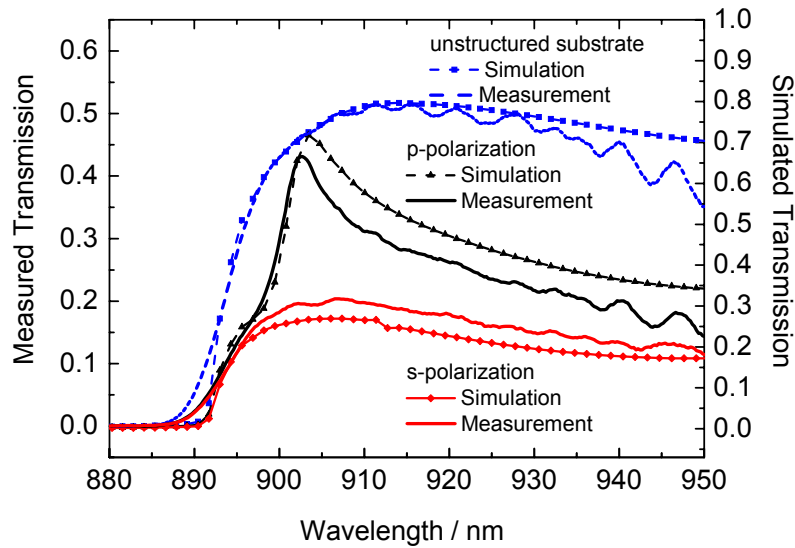


Fig. 14. Comparison of FDTD simulations and measured transmission of a 80 nm thick silver grating on top of GaAs/AlAs heterostructure.

5. CONCLUSION AND OUTLOOK

We demonstrated the simulation, fabrication and optical characterization of nano-structured metal gratings. We optimized metal grating parameters for plasmonic enhanced transmission of light through gratings on top of GaAs/AlAs/GaAs heterostructures. Using laser interference lithography we were able to produce metal gratings with periodicities of 540 nm and thicknesses up to 100 nm. We found good consistency between our simulations and the measured transmission of these structures, which encourages us to intensify the efforts for fabrication of 170-nm-thick metal gratings.

For the future we expect enhanced efficiency of light emitting diodes using metal gratings as top electrodes. According to our simulations, we estimate an improvement of 35 %.

ACKNOWLEDGEMENTS

The authors gratefully acknowledge financial support from the German Federal Ministry of Education and Research BMBF within the project ‘Plasmonisch optimierte LEDs’ (FKZ 13N9153) and by the DFG Research Center for Functional Nanostructures (CFN).

REFERENCES

- [1] M. Liu, B. Rong, and H. Salemin, "Evaluation of LED application in general lighting", *Optical Engineering* 46(7), 074002 (2007)
- [2] Y. Narukawa, J. Narita, T. Sakamoto, T. Yamada, H. Narimatsu, M. Sano, and T. Mukai, "Recent progress of high efficiency white LEDs", *Physica Status Solidi (a)*, 204, No. 6, 2087–2093 (2007)
- [3] T. Oder, K. Kim, J. Lin, and H. Jiang, "III-nitride blue and ultraviolet photonic crystal light emitting diodes", *Applied Physics Letters* 84(4), 466-468 (2004)
- [4] J. Wierer, M. Krames, J. Epler, N. Gardner, M. Craford, J. Wendt, J. Simmons, and M. Sigalas, "InGaN/GaN quantum-well heterostructure light-emitting diodes employing photonic crystal structures", *Applied Physics Letters* 84(19), 3885-3887 (2004)
- [5] E. Schubert, Y.-H. Wang, A. Cho, L.-W. Tu, and G. Zyzdik, "Resonant cavity light-emitting diode", *Applied Physics Letters* 60(8), 921-923 (2004)
- [6] M. Krames, M. Ochiai-Holcomb, G. Höfler, C. Carter-Coman, E. Chen, I.-H. Tan, P. Grillot, N. Gardner, H. Chui, J.-W. Huang, S. Stockman, F. Kish, M. Craford, T. Tan, C. Kocot, M. Hueschen, J. Posselt, B. Loh, G. Sasser, and D. Collins, "High-power truncated-inverted-pyramid $(\text{Al}_x\text{Ga}_{1-x})_{0.5}\text{In}_{0.5}\text{P}/\text{GaP}$ light-emitting diodes exhibiting >50 external quantum efficiency", *Applied Physics Letters* 75(16), 2365-2367 (1999)
- [7] S. Gianordoli, R. Hainberger, A. Köck, N. Finger, E. Gornik, C. Hanke and L. Korte, "Optimization of the emission characteristics of light emitting diodes by surface plasmons and surface waveguide modes", *Applied Physics Letters* 77(15), 2295-2297 (2000)
- [8] K. Okamoto, I. Niki, A. Shvartser, Y. Narukawa, T. Mukai, and A. Scherer, "Surface-plasmon-enhanced light emitters based on InGaN quantum wells", *Nature Materials* 3(9), 601-605 (2004)
- [9] D. Lepage, and J. Dubowski, "Surface plasmon assisted photoluminescence in GaAs–AlGaAs quantum well microstructures", *Applied Physics Letters* 91(16), 163106 (2007)
- [10] D.-M. Yeh, C.-F. Huang, C.-Y. Chen, Y.-C. Lu, and C. C. Yang, "Surface plasmon coupling effect in an InGaN/GaN single-quantum-well light-emitting diode", *Applied Physics Letters* 91(17), 171103 (2007)
- [11] M.-K. Kwon, J.-Y. Kim, B.-H. Kim, I.-K. Park, C.-Y. Cho, C. Byeo, and S.-J. Park, "Surface-plasmon-enhanced light-emitting diodes", *Advanced Materials* 20(7), 1253 (2008)
- [12] W. Barnes, A. Dereux, and T. Ebbesen, "Surface plasmon subwavelength optics", *Nature* 424(6950), 824-830 (2003)
- [13] E. Kreschmann, and H. Raether, *Z. Naturforsch.* 23A, 2135 (1968)
- [14] T. Ebbesen, H. Lezec, H. Ghaemi, T. Thio, and P. Wolff, "Extraordinary optical transmission through sub-wavelength hole arrays", *Nature* 391 (6668), 667-669 (1998)
- [15] M. Harries, and H. Summers, "Directional control of light-emitting-diode emission via a subwavelength-apertured metal surface" *IEEE Photonics Technology Letters* 18 (21), 2197-2199 (2006)
- [16] S. Wedge, A. Giannattasio, and W. Barnes, "Surface plasmon-polariton mediated emission of light from top-emitting organic light-emitting diode type structures", *Organic Electronics* 8(2), 136-147 (2007)
- [17] N. Efremow, N. Economou, K. Bezjian, S. Dana, and H. Smith, "A simple technique for modifying the profile of resist exposed by holographic lithography", *Journal of Vacuum Science and Technology* 19(4), 1234-1237 (1981)